

Cavity-photon controlled thermoelectric transport through a quantum wire

Nzar Rauf Abdullah,^{1,2,*} Chi-Shung Tang,³ Andrei Manolescu,⁴ and Vidar Gudmundsson^{2,†}

¹*Physics Department, Faculty of Science and Science Education,
School of Science, University of Sulaimani, Kurdistan Region, Iraq*

²*Science Institute, University of Iceland, Dunhaga 3, IS-107 Reykjavik, Iceland*

³*Department of Mechanical Engineering, National United University, 1, Lienda, Miaoli 36003, Taiwan*

⁴*Reykjavik University, School of Science and Engineering, Menntavegur 1, IS-101 Reykjavik, Iceland*

We investigate the influence of a quantized photon field on thermoelectric transport of electrons through a quantum wire embedded in a photon cavity. The quantum wire is connected to two electron reservoirs at different temperatures leading to a generation of a thermoelectric current. The transient thermoelectric current strongly depends on the photon energy and the number of photons initially in the cavity. Two different regimes are studied, off-resonant and resonant polarized fields, with photon energy smaller than, or equal to the energy spacing between some of the lowest states in the quantum wire. We observe that the current is inverted for the off-resonant photon field due to participation of photon replica states in the transport. A reduction in the current is recorded for the resonant photon field, a direct consequence of the Rabi-splitting.

INTRODUCTION

Thermoelectric transport is a subject of intense study for future energy harvesting devices [1, 2]. Low-dimensional electronic systems have a potential to improve thermoelectric efficiency compared to bulk electronic materials due to their highly peaked density of states for system sizes in the range of nanometers [3]. A thermoelectric current (TEC) can be generated by a temperature gradient ΔT in an electronic systems. In the linear response regime, the temperature gradient approaches zero and the thermoelectric efficiency is characterized by the dimensionless figure of merit ZT [4]. In the non-linear response regime, the thermoelectric efficiency is represented by the bias voltage ΔV generated by ΔT [5]. In both regimes, the thermal efficiency can be high in nanodevices.

Since the 1990's, the thermoelectric transport has been investigated in several quantum systems, such as single quantum dots [6–8], double quantum dots [9], and quantum wires [10]. The Coulomb interaction between charge carriers influences the thermal transport through a quantum dot and forms plateaus in the TEC [11]. The thermoelectric effect through a serial double quantum dot weakly coupled to ferromagnetic leads has been investigated, and the influence of temperature and inter-dot tunneling on the figure of merit has been demonstrated [12].

Another interesting aspect of this issue is the importance of photon radiation to control thermal transport. Recently, time-dependent photon radiation has been used to enhance the heat and thermoelectric transport [13, 14]. Photonic heat current through an arbitrary circuit element coupled to two dissipative reservoirs has been explored at finite temperatures [15]. Transfer of heat via photons between two metals is reported to study photonic power where the metals are coupled by a circuit containing linear reactive impedance [16].

Here, we describe the TEC in a quantum wire coupled to two electron reservoirs with different temperatures and the same chemical potential. The temperature gradient causes electron flow from the leads to the quantum wire and vice versa. In addition, the quantum wire is coupled to a cavity

field with photons polarized in the direction of electron propagation in the quantum wire. A generalized master equation is used to calculate the time-dependent evolution of electrons in the quantum wire [17, 18]. We show how TEC can be controlled by cavity parameters such as the photon energy in off-resonant and on-resonant photon fields.

METHOD AND THEORY

We assume a short quantum wire is formed in a two-dimensional electron gas in the x - and y -plane. The quantum wire is hard-wall confined at the ends in the x -direction and parabolically confined in the y -direction. The wire with length $L_x = 150$ nm is weakly coupled to two leads held at different temperatures. The total system is exposed to an external perpendicular static magnetic field $B = 0.1$ T with cyclotron energy $\hbar\omega_c = 0.172$ meV. The transverse confinement energy of the electrons in the quantum wire is equal to that of the leads $\hbar\Omega_0 = \hbar\Omega_l = 2.0$ meV, where l refers to the left (L), or the right (R) lead. The effective confinement frequency is $\Omega_w = \sqrt{\Omega_0^2 + \omega_c^2}$. The photons in the cavity are linearly polarized in the x -direction. We tune the photon energy, and the number of photons initially in the cavity to control the transient TEC in the quantum wire.

Fig. 1 shows a schematic diagram of the quantum wire (white color) coupled to the left lead (red color) with temperature T_L , and the right lead (blue color) with temperature T_R . The red zigzag arrows indicate the polarized photon field.

The time-evolution of the many-body density operator of the system is governed by the Liouville-von Neumann equation. Due to its complexity a generalized master equation for the reduced density operator is derived by projecting the system description onto the central system, the short quantum wire [19, 20]. As we are dealing with off- and on-resonance processes we include both the para- and the diamagnetic electron-photon interactions without the rotating wave approximation [21]. The electron-electron and the electron-photon interactions are treated by exact diagonalization in ap-

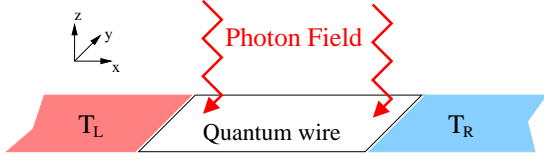


FIG. 1. (Color online) Schematic diagram of a quantum wire (white color) connected to a left lead (pink color) with temperature T_L , and a right lead (blue color) with temperature T_R . The photon field is represented by the red zigzag arrows.

proportionately truncated Fock-spaces. Our interest in the transient behavior of the system requires a non-Markovian approach valid to a weak coupling of the leads to the central system [22].

Off-resonance photon field

In this section, we assume the photon energy is smaller than the energy spacing between the three lowest energy states of the quantum wire. For instance, the photon energy is $\hbar\omega_\gamma < E_1 - E_0$ where $E_0(E_1)$ is the energy of the ground state (first-excited state) of the quantum wire, respectively.

Figure 2(a) shows the energy spectrum versus electron-photon coupling strength g_γ , where 0ES (golden circles) are zero-electron states, 1ES (blue squares) are one-electron states and the horizontal lines (red lines) indicate the location of the resonance condition for the lowest three one-electron states with the chemical potentials of the leads, $\mu_L = \mu_R = E_\mu$, at $g_\gamma = 0$. We start with no electron-photon coupling,

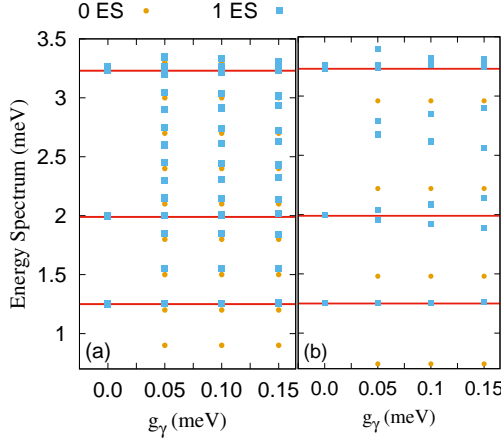


FIG. 2. (Color online) Energy spectrum of the quantum wire versus electron-photon coupling strength g_γ . 0ES (golden circles) are zero-electron states, 1ES (blue squares) are one-electron states and the horizontal lines (red lines) display the location of the resonances of the leads with the three lowest one-electron states in the case of off-resonance (a) and resonance (b) photon field. The photon energy is $\hbar\omega_\gamma = 0.3$ meV, $N_\gamma = 2$, and the photons are linearly polarized in the x -direction. The magnetic field is $B = 0.1$ T, and $\hbar\Omega_0 = 2.0$ meV.

$g_\gamma = 0.0$ meV. In this case, we concentrate our attention

on the three lowest states in a selected range of the energy spectrum: the ground state, the first-excited state, and the second-excited state with energy values $E_0 = 1.25$ meV, $E_1 = 1.99$ meV, and $E_2 = 3.23$ meV, respectively. In the presence of electron-photon coupling with off-resonant photon field, photon replicas of the above mentioned three states are formed. The separation between the photon replica states is approximately equal to the photon energy for the selected values of the electron-photon coupling strength used here. The photon replicas play an important role in the thermoelectric transport.

Figure 3 demonstrates the TEC (a) and the occupation (b) for the three lowest states of the quantum wire in the case of no electron-photon coupling, $g_\gamma = 0.0$ meV. We fix the temperature of the right lead at $k_B T_R = 0.05$ meV, and vary the temperature of the left lead to $k_B T_L = 0.1$ (blue diamonds), 0.15 (green squares) and 0.25 meV (golden circles). In Fig. 3(a)

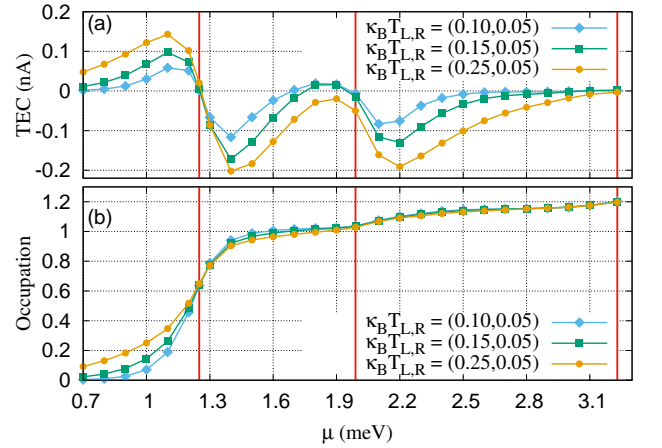


FIG. 3. (Color online) TEC (a), and occupation (b) as functions of the chemical potential $\mu = \mu_L = \mu_R$ plotted at time $t = 220$ ps. The temperature of the right lead is fixed at $T_R = 0.58$ K implying thermal energy 0.05 meV, and varying the temperature of the left lead to $T_L = 1.16, 1.742$ and 2.901 K implying thermal energies 0.1 (blue diamonds), 0.15 (green squares), and 0.25 meV (golden circles), respectively. The red vertical lines show the resonance condition for the ground state at $\mu = 1.25$ meV, the first-excited state at $\mu = 1.99$ meV, and the second-excited state at $\mu = 3.23$ meV, respectively. The magnetic field is $B = 0.1$ T, and $\hbar\Omega_0 = 2.0$ meV.

the TEC as a function of chemical potential $\mu = \mu_L = \mu_R$ is plotted at time $t = 220$ ps. At this time point the system is in the late transient regime very close to a steady state. The concept of a TEC can be loosely explained as being related to the Fermi functions of the leads. The TEC is zero in the following cases: half filling, where the Fermi function of the leads is equal to 0.5, and integer filling, where the Fermi function of the leads is either 0 or 1 [6].

For instance, the TEC is zero at $\mu = 1.25$ meV corresponding to approximately half filling of the ground state as is shown in Fig. 3(b). In addition, the TEC is again zero at $\mu = 0.7$ and 1.7 meV for the integer filling of occupation 0

and 1, respectively.

In the presence of a higher temperature of the left lead at $k_B T_L = 0.25$ meV, a shifting in the TEC is observed for the first-excited state at $\mu = 1.99$ meV. The current deviation occurs due to an increased thermal smearing at the higher temperature. In this case, both the ground state and the first-excited state participate in the electron transport at $\mu = 1.99$ meV. Therefore, the current becomes negative, instead of the zero value at a lower temperature.

Furthermore, we notice that the second-excited state of the quantum wire is in resonance with the second subband of the leads. The wavefunction of the second-excited state of the central system is symmetric in the y -direction while the wavefunctions of the second subband of the leads are anti-symmetric in the y -direction. The electron transport from a symmetric to an anti-symmetric state or vice versa is not allowed due to the geometry sensitive function that describes the coupling between the quantum wire and the leads [17, 23]. Therefore, a plateau in the current is formed for the second-excited state around $\mu = 3.23$ meV.

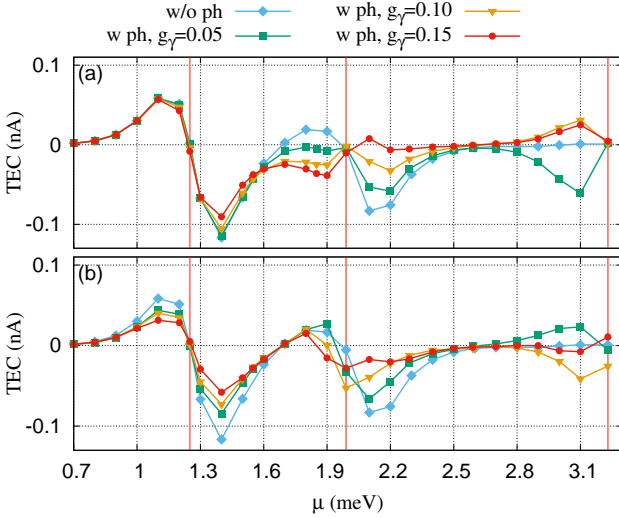


FIG. 4. (Color online) TEC as a function of the chemical potential $\mu = \mu_L = \mu_R$ plotted at time $t = 220$ ps without photon cavity $g_\gamma = 0.0$ meV (blue diamonds), and with photon cavity for the electron-photon coupling strength $g_\gamma = 0.05$ (green squares), 0.10 (golden triangles), and 0.15 meV (red circles) in the case of off-resonance (a) and resonance (b) photon field. The photon energy is $\hbar\omega_\gamma = 0.3$ meV and the photons are linearly polarized in the x -direction. The temperature of the left (right) lead is fixed at $T_L = 1.16$ K ($T_R = 0.58$ K) implying thermal energy $k_B T_L = 0.10$ meV ($k_B T_R = 0.05$ meV), respectively. The magnetic field is $B = 0.1$ T, and $\hbar\Omega_0 = 2.0$ meV.

Now, we assume the quantum wire is embedded in a photon cavity with a photon mode of energy $\hbar\omega_\gamma = 0.3$ meV, and the cavity initially contains two photons $N_\gamma = 2$. The photons are linearly polarized in the x -direction. The photon energy is smaller than the energy spacing between the ground state and the first-excited state on one hand, and the first-excited state and the second-excited state on the other hand. This means

that the system is off-resonant with respect to the photon field. The energy spectrum of the quantum wire embedded in the cavity with off-resonant photon field was shown in Fig. 2(a).

The TEC as a function of the chemical potential of the leads is displayed in Fig. 4(a) for the system without a photon cavity $g_\gamma = 0.0$ meV (blue diamonds), and with a photon cavity for the electron-photon coupling strength $g_\gamma = 0.05$ (green squares), 0.10 (golden triangles), and 0.15 meV (red circles) in the case of off-resonant photon field at time $t = 220$ ps. We observe that the current through the ground state is almost unchanged in the presence of a photon cavity, but the characteristics of the TEC of the first-excited state and the second-excited state are drastically modified. The influence of cavity photon field is to invert the TEC from ‘positive’ to ‘negative’ values or vice versa around the first-excited state at $\mu = 1.99$ meV. The two photon replica of the ground state at $\mu = 1.84$ meV contributes to the electron transport with the first-excited state leading to the current flip from ‘positive’ to ‘negative’ values. In addition, the two photon replica of the first-excited state around $\mu = 2.59$ meV becomes active in the transport. Therefore, the TEC is inverted from ‘negative’ to ‘positive’ values around $\mu = 2.1$ meV.

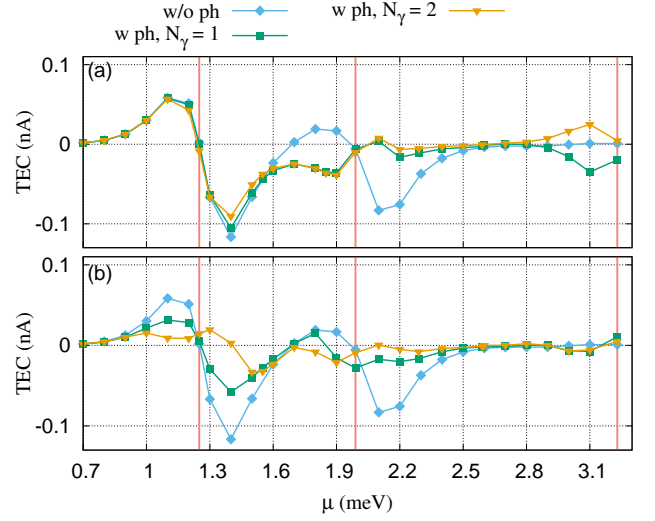


FIG. 5. (Color online) TEC as a function of the chemical potential $\mu = \mu_L = \mu_R$ plotted at time $t = 220$ ps without photon cavity $g_\gamma = 0.0$ meV (blue diamonds), and with photon cavity initially containing one photon $N_\gamma = 1$ (green squares) and two photons $N_\gamma = 2$ (golden triangles) in the case of off-resonance (a) and resonance (b) photon field. The photon energy is $\hbar\omega_\gamma = 0.3$ meV and the photons are linearly polarized in the x -direction. The temperature of the left (right) lead is fixed at $T_L = 1.16$ K ($T_R = 0.58$ K) implying thermal energy $k_B T_L = 0.10$ meV ($k_B T_R = 0.05$ meV), respectively. The magnetic field is $B = 0.1$ T, and $\hbar\Omega_0 = 2.0$ meV.

The electron transport is affected around the second-excited state in the presence of the photon cavity as is shown in Fig. 4(a). This is because the two photon replica of the first-excited state is getting into resonance with the second subband of the leads. The two photon replica of the first-excited state has an

anti-symmetric wavefunction in the y -direction and the wavefunctions of the second subband are anti-symmetric as well. Consequently, the electrons transfer from the second subband of the leads to the two photon replica of the first-excited state of the quantum wire. A TEC is thus generated.

The effects of the initial number of photons on the TEC is shown in Fig. 5. The off-resonance system (Fig. 5(a)) is rather insensitive to the exact number of photons in the low energy regime. This is because both one and two photon replica states are close to each other in the off-resonant photon field. The thermal smearing leads to participation of both states in the electron transport. Therefore, the selected initial photon number in the cavity does not influence the TEC.

On-resonance photon field

In this section we assume the photon energy is approximately equal to the energy spacing between the ground-state and the first-excited state $\hbar\omega_\gamma \cong E_1 - E_0$. The system under consideration is in resonance with the photon field. The photon energy is assumed to be $\hbar\omega_\gamma = 0.74$ meV and the cavity initially contains one photon, $N_\gamma = 1$.

The energy spectrum of the quantum wire as a function of the electron-photon coupling strength g_γ in the presence of the resonant photon field is displayed in Fig. 2(b), where OES (golden circles) are zero-electron states and 1ES (blue squares) are one-electron states. The horizontal lines (red lines) display the energy of possible transport resonances. In the case of no electron-photon coupling at $g_\gamma = 0.0$ meV the three states mentioned in the previous section are again found in the selected range of energy. In the presence of the cavity field the one photon replica of the ground state is observed near the first-excited state at $g_\gamma = 0.05$ meV.

Increasing the electron-photon coupling strength to $g_\gamma = 0.15$ meV, the one photon replica of the ground state is lowered in energy and the first-excited state shifts up. Therefore, the separation between these two states increases. Similar splitting in the energy spectrum can be seen in the higher energy states between 2.5-3.0 meV. The splitting is the Rabi-splitting.

Figure 4(b) shows TEC versus chemical potential at time $t = 220$ ps without a photon cavity $g_\gamma = 0.0$ meV (blue diamonds) and with a photon cavity for the electron-photon coupling strength $g_\gamma = 0.05$ (green squares), 0.10 (golden triangles), and 0.15 meV (red circles) in the case of resonant of the photon field. The temperature of the left lead is fixed at $T_L = 1.16$ K implying thermal energy $k_B T_L = 0.10$ meV and the temperature of the right lead is assumed to be $T_R = 0.58$ K with thermal energy $k_B T_R = 0.05$ meV.

In the resonant photon field, a reduction in the TEC is observed with increasing electron-photon coupling strength. For $g_\gamma = 0.05$ meV, the following three states contribute to the electron transport at $\mu = 1.10$ meV with ‘positive’ current, and at $\mu = 1.40$ meV with ‘negative’ current: The ground state, the one photon replica of the ground state, and the

first-excited state. Increasing the electron-photon coupling strength to $g_\gamma = 0.15$ meV the first-excited state shifts up and does not participate in the electron transport. Therefore, the TEC is suppressed.

The TEC decreases at $\mu = 1.90$ and 2.10 meV around the first-excited state. The current suppression is due to participation of the one photon replica of the first-excited state with the energy 2.65 meV at $g_\gamma = 0.05$ meV. But at the higher electron-photon coupling strength $g_\gamma = 0.15$ meV the one photon replica of the first-excited state is not active in the transport. This is because it moves up for high electron-photon coupling strength. Consequently, the TEC drops down. This reduction in the thermoelectric current is a direct consequence of the Rabi-splitting of the energy levels of the system. Earlier, we have established dynamic effects of the Rabi-splitting on the transport current through the system at a finite bias voltage [24]. The electrons are getting active in the transport around the second-excited state. The activation of the electron transport there is due to the symmetry properties of the one photon replica of the first-excited state. We have verified that the TEC flattens out as the temperature of both leads is increased keeping their temperature difference constant.

Opposite to the off-resonant system, the initial photon number in the resonant system can change the TEC substantially, as is seen in Fig. 5(b). The reason is the larger separation between photon replica states here. Consequently, the place of the active photon replicas in the energy spectrum is important and the initial photon number influences the TEC.

CONCLUSIONS

We studied numerically the thermoelectric transport properties of a short quantum wire interacting with either off- or on-resonant cavity-photon field. The quantum wire is assumed to be connected to two electron reservoirs with different temperatures. The temperature gradient accelerates electrons from the leads to the quantum wire creating a thermoelectric current. We showed that a plateau in the current is formed due to symmetry properties of the energy states of the quantum wire and the leads in the case of no cavity photon field. By applying a linearly polarized photon field, the photon replica states result in an inverted thermoelectric transport in the off-resonance regime. Moreover, in the on-resonant photon field the effects of a Rabi-splitting in the energy spectrum appears leading to a reduction in the thermoelectric current. In both regimes, the current plateaus that were formed in the absence of a photon field are removed due to the generation of photon replica states. Our results point to new opportunities to experimentally control thermoelectric transport properties of nanodevices with a cavity photon field.

Financial support is acknowledged from the Icelandic Research and Instruments Funds, and the Research Fund of the University of Iceland. The calculations were carried out on the Nordic High Performance Computer Center in Iceland. We

acknowledge the Nordic network NANOCONTROL, project No.: P-13053, and the Ministry of Science and Technology, Taiwan through Contract No. MOST 103-2112-M-239-001-MY3.

* nzar.r.abdullah@gmail.com

† vidar@hi.is

- [1] A. Shakouri. Recent Developments in Semiconductor Thermoelectricity Physics and Materials. *Annu. Rev. Mater. Res.*, 41:399, 2011.
- [2] A. Majumdar. Thermoelectricity in Semiconductor Nanostructure. *Science*, 303:777–778, 2004.
- [3] Joseph P. Heremans, Vladimir Jovovic, Eric S. Toberer, Ali Saramat, Ken Kurosaki, Anek Charoenphakdee, Shinsuke Yamanaka, and G. Jeffrey Snyder. Enhancement of Thermoelectric Efficiency in PbTe by Distortion of the Electronic Density of States. *Science*, 321(5888):554–557, 2008.
- [4] L. D. Hicks and M. S. Dresselhaus. Effect of quantum-well structures on the thermoelectric figure of merit. *Phys. Rev. B*, 47:12727–12731, May 1993.
- [5] Olli-Pentti Saira, Matthias Meschke, Francesco Giazotto, Alexander M. Savin, Mikko Möttönen, and Jukka P. Pekola. Heat Transistor: Demonstration of Gate-Controlled Electronic Refrigeration. *Phys. Rev. Lett.*, 99:027203, Jul 2007.
- [6] C. W. J. Beenakker and A. A. M. Staring. Theory of the thermopower of a quantum dot. *Phys. Rev. B*, 46:9667–9676, Oct 1992.
- [7] A. V. Andreev and K. A. Matveev. Coulomb Blockade Oscillations in the Thermopower of Open Quantum Dots. *Phys. Rev. Lett.*, 86:280–283, Jan 2001.
- [8] S. Fahlvik Svensson, A. I. Persson, E. A. Hoffmann, N. Nakpathomkun, H. A. Nilsson, H. Q. Xu, L. Samuelson, and H. Linke. Lineshape of the thermopower of quantum dots. *New Journal of Physics*, 14(3):033041, 2012.
- [9] R. Świrkowicz, M. Wierzbicki, and J. Barnaś. Thermoelectric effects in transport through quantum dots attached to ferromagnetic leads with noncollinear magnetic moments. *Phys. Rev. B*, 80:195409, Nov 2009.
- [10] D. A. Broido and T. L. Reinecke. Theory of thermoelectric power factor in quantum well and quantum wire superlattices. *Phys. Rev. B*, 64:045324, Jul 2001.
- [11] K. Torfason, A. Manolescu, S. I. Erlingsson, and V. Gudmundsson. Thermoelectric current and Coulomb-blockade plateaus in a quantum dot. *Physica E*, 53:178–185, 2013.
- [12] M. Bagheri Tagani and H. Rahimpour Soleimani. Thermoelectric effects in a double quantum dot system weakly coupled to ferromagnetic leads. *Solid State Communications*, 152(10):914–918, 2012.
- [13] Xiaobin Chen, Dongping Liu, Wenhui Duan, and Hong Guo. Photon-assisted thermoelectric properties of noncollinear spin valves. *Phys. Rev. B*, 87:085427, Feb 2013.
- [14] Allon I. Hochbaum, Renkun Chen, Raul Diaz Delgado, Wenjie Liang, Erik C. Garnett, Mark Najarian, Arun Majumdar, and Peidong Yang. Enhanced thermoelectric performance of rough silicon nanowires. *Nature*, 455:778–781, 2008.
- [15] Teemu Ojanen and Antti-Pekka Jauho. Mesoscopic Photon Heat Transistor. *Phys. Rev. Lett.*, 100:155902, Apr 2008.
- [16] L. M. A. Pascal, H. Courtois, and F. W. J. Hekking. Circuit approach to photonic heat transport. *Phys. Rev. B*, 83:125113, Mar 2011.
- [17] N. R. Abdullah, C. S. Tang, A. Manolescu, and V. Gudmundsson. Electron transport through a quantum dot assisted by cavity photons. *Journal of Physics: Condensed Matter*, 25:465302, 2013.
- [18] N. R. Abdullah, C. S. Tang, A. Manolescu, and V. Gudmundsson. Coherent transient transport of interacting electrons through a quantum waveguide switch. *Journal of physics: Condensed matter*, 27:015301, 2015.
- [19] S. Nakajima. On quantum theory of transport phenomena steady diffusion. *Prog. of Theor. Phys.*, 20:948, 1958.
- [20] Robert Zwanzig. Ensemble Method in the Theory of Irreversibility. *The Journal of Chemical Physics*, 33(5):1338–1341, 1960.
- [21] Olafur Jonasson, Chi-Shung Tang, Hsi-Sheng Goan, Andrei Manolescu, and Vidar Gudmundsson. Nonperturbative approach to circuit quantum electrodynamics. *Phys. Rev. E*, 86:046701, Oct 2012.
- [22] V. Gudmundsson, O. Jonasson, Th. Arnold, C.-S. Tang, H.-S. Goan, and A. Manolescu. Stepwise introduction of model complexity in a general master equation approach to time-dependent transport. *Fortschr. Phys.*, 61:305, 2013.
- [23] V. Gudmundsson, C. Gainar, C.-S. Tang, V. Moldoveanu, and A. Manolecu. Time-dependent transport via the generalized master equation through a finite quantum wire with an embedded subsystem. *New J. Phys.*, 11:113007, 2009.
- [24] Vidar Gudmundsson, Anna Sitek, Pei-yi Lin, Nzar Rauf Abdullah, Chi-Shung Tang, and Andrei Manolescu. Coupled collective and Rabi oscillations triggered by electron transport through a photon cavity. *ACS Photonics*, 2:930, 2015.